

# Simulation of Hydrodynamic Dispersion in Gas/Liquid Microreactors

S. Hardt, F. Doffing and H. Pennemann

Institut für Mikrotechnik Mainz GmbH, Carl-Zeiss-Str. 18-20,  
D-55129 Mainz, Germany, hardt@imm-mainz.de

## ABSTRACT

Dispersion and spreading of concentration signals in gas/liquid microreactors is studied with methods of computational fluid dynamics (CFD). It is shown that conventional reactor designs exhibit a broad residence-time distribution due to convective signal dispersion. This result is supported by experiments monitoring the transport of a liquid plug introduced into the microreactor by a micro-dispenser. A new reactor design is proposed which exhibits a more favorable velocity profile by guiding the liquid stream over alternating platelets. With simulations based on the volume-of-fluid (VOF) method it is shown that a thin, continuous liquid film forms inside the reactor. Subsequently, the transport of concentration fields described by a convection-diffusion equation is studied. It is found that, due to the approximate plug-flow character of fluid motion within this film, concentration signals experience significantly lower dispersion than in the conventional design. The new reactor design will provide the basis of a new class of gas/liquid microreactors to be developed at the Institute of Microtechnology Mainz.

**Keywords:** Microreactors, hydrodynamic dispersion, computational fluid dynamics, volume-of-fluid method.

## 1 INTRODUCTION

Due to an increase of specific interfacial area and a reduction of diffusion paths, microreactors offer unique opportunities for fast gas/liquid reactions. At the Institute of Microtechnology Mainz (IMM) two classes of gas/liquid microreactors have been developed. A falling film reactor [1] and a micro bubble column [2]. In a number of experiments it was proven that in such microreactors mass-transfer limited reactions can be carried out with higher conversion and selectivity than in conventional equipment [1]. Moreover, space-time yields were found to exceed those obtained with standard reactors by orders of magnitude [1] and significantly higher specific interfacial areas were measured [2].

Fig. 1 shows the falling film microreactor disassembled into its three main components. The reaction occurs on a microstructured reaction plate containing 64 grooves of 300  $\mu\text{m}$  width and 100  $\mu\text{m}$  depth. A liquid film is transported within the grooves by action of gravitational forces. Above the liquid a gas stream flows either in co-current or in counter-current direction, allowing chemical reactions to

occur between the two phases. The liquid film thickness, typically of the order of several tens of a micron, is controlled via the mass flow fed to the reactor.

The falling film reactor allows to carry out gas/liquid reactions under more well defined conditions than in conventional equipment. Potential application areas are catalyst screening as well as production of fine chemicals and corresponding process development. For these applications, a narrow residence time of tracers introduced into the liquid phase is of paramount importance. In the following the corresponding problem of signal dispersion is investigated using CFD methods.

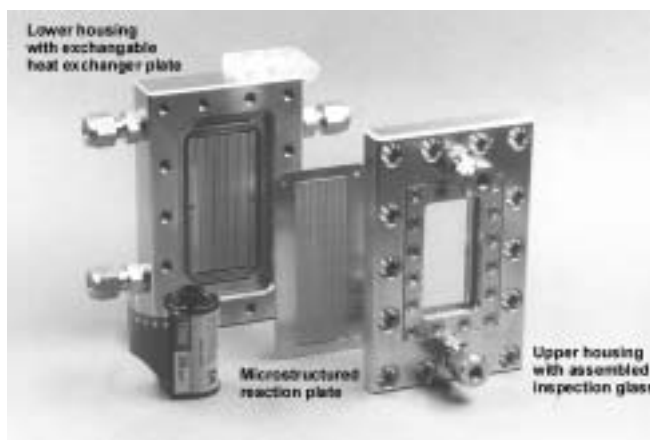


Figure 1: Falling film microreactor. The reaction plate contains micro-grooves for the liquid film.

## 2 HYDRODYNAMIC DISPERSION IN THE FALLING FILM REACTOR

For the measurement of reaction kinetics of gas/liquid reactions, experimental conditions should ensure a well defined contact time between the two phases. On the other hand, in production processes side reactions should be suppressed, again translating into a demand for a narrow residence time distribution. In order to investigate the dispersion of concentration signals in the falling film reactor, CFD simulations based on the finite-volume method were performed. Furthermore, experiments were conducted studying the spreading of water blue tracers inside the micro-grooves.

### 2.1 CFD Simulations

The detailed geometrical shape of the micro-grooves

depends on the specific microstructuring technique employed for fabrication of the reaction plate. For reasons of chemical and thermal resistance, stainless steel was chosen as reactor material. When structuring the plate by electric discharge machining, nearly rectangular channel cross sections are obtained. In contrast to that, wet chemical etching produces rounded shapes. In order to measure the exact geometry of the grooves produced by wet chemical etching, the reaction plate surface was scanned with a laser interferometer (UBM microfocus, UBM, Germany). The obtained surface profiles were imported into the CFD preprocessor as starting point for the geometrical model.

The CFD model used is based on a finite volume approach. The incompressible Navier-Stokes equation in combination with the convection-diffusion equation for species concentration was solved. If not stated otherwise, the SIMPLEC algorithm for velocity-pressure coupling, first order hybrid differencing for the momentum equation and the second-order QUICK scheme [3] for species concentration in combination with the CFX4 flow solver from AEA Technology were used.



Figure 2: Flow velocity contours in EDM machined (above) and etched grooves (below). High velocities are indicated in light colors.

In order to reduce the computational complexity of the model, a few simplifying assumptions were made. At low gas velocities, the shear force exerted by the gas on the liquid surface is negligible. In this case, the gas/liquid interface can be treated as a symmetry boundary with vanishing momentum flux. Furthermore, at low liquid flow velocities the interface will assume a stationary shape with constant curvature minimizing the free energy of the system. In order to check the validity of this assumption, the kinetic energy  $E_{kin}$  of a moving liquid plug has to be compared with its surface energy  $E_s$

$$\frac{E_{kin}}{E_s} \approx \frac{1}{4} \frac{\rho h u^2}{\sigma} = \frac{1}{4} We, \quad (1)$$

with  $\rho$  being the liquid density,  $u$  its velocity,  $\sigma$  the surface tension,  $h$  the depth of the grooves and  $We$  the Weber number. For characteristic flow velocities in the mm/s range, typically Weber numbers below  $10^{-3}$  are obtained, indicating the validity of the above assumption. Thus, in this dynamical range the computational domain can be restricted to the space occupied by the liquid. This domain is bounded by a curved surface representing the gas/liquid interface and another surface representing the channel walls.

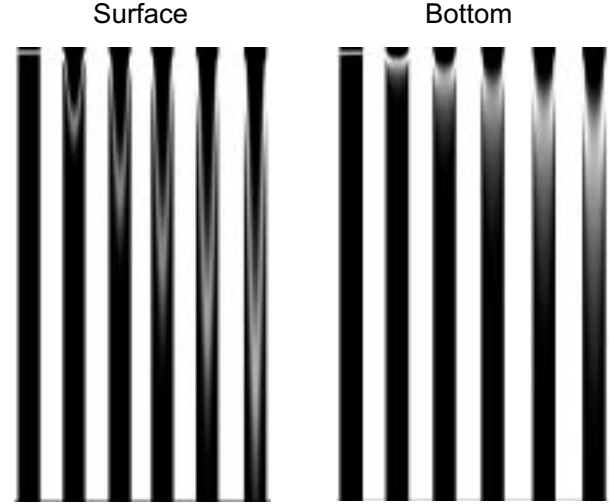


Figure 3: Spreading of a concentration signal in an etched groove as seen on the gas/liquid interface (left) and on the bottom of the groove (right).

Fig. 2 displays a cross section through the liquid inside the grooves, where the velocity profile a rectangular cross section (above) is compared that in etched channels. Complete filling of the grooves (corresponding to maximum flow rate), liquid properties of ethanol at 20 °C and a contact angle to stainless steel of 30° was assumed. Measured contact angles for organic liquid/metal systems may depend on certain details as surface roughness, but are usually small. As apparent from the figure, the velocity profile displays a double or single maximum, depending on the channel cross section. The computed flow velocities are in the range of millimeters per second.

In Fig. 3 the spreading of a concentration signal in an etched groove of the falling film reactor is shown at equally spaced time steps. For this purpose the convection-diffusion equation for the concentration field was solved for a prescribed velocity field obtained from the previous simulations. A value of the diffusion constant as low as  $10^{-9}$  m<sup>2</sup>/s was chosen, as characteristic for diffusion in liquids. By comparison to a simulation run with zero diffusion constant it was shown that the spreading of the signal is not dominated by numerical diffusion. This suppression of numerical artifacts is due to grid cells being strictly aligned with the flow velocity vectors [4]. The results show that the spreading of the signal is attributed to convective rather

than diffusive effects, as could have been found earlier by computing characteristic Peclet numbers of the flow. The computed signal dispersion is considerable and will, e.g., diminish the usefulness of the reactor for catalyst screening.

## 2.2 Experiments

In order to study signal spreading experimentally, droplets of water blue solution were introduced into the grooves using a micro-dispenser developed at IMM. The micro-dispenser was operated such that a droplet of 230  $\mu\text{m}$  diameter impinged on the downward flowing liquid in a single micro-groove. The experiments were done with an ethanol film at flow velocities of several mm/s, corresponding to the flow rates assumed in the simulations. The spreading of the dye was recorded with a video camera. In Fig. 4 four snapshots are shown which display the spatial evolution of the concentration signal. The arrows indicate the approximate width of the signal. Initially, the dye is contained in a narrow plug (left side of the figure) which spreads very fast while it moves downwards, thus increasing in length and getting diluted. As opposed to the simulation, the experiment only gives information averaged over the thickness of the liquid film. However, both experiment and simulation clearly indicate that concentration signals get dispersed significantly within the micro-grooves, thus resulting in a comparatively broad residence-time distribution.

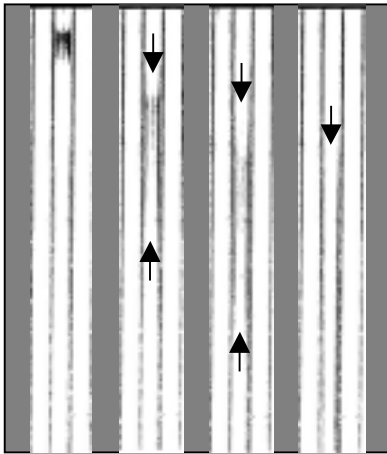


Figure 4: Video images displaying the spreading of a water blue droplet in a micro-groove of the falling film reactor

## 3 OPTIMIZATION OF THE REACTOR GEOMETRY

A modified reactor design has been developed and evaluated using CFD methods, especially with respect to hydrodynamic dispersion. In this reactor design the reaction plate is replaced by alternating platelets, with an extension in flow direction of typically less than a few millimeters. The platelets are arranged in such a way that the regions of

the liquid film in contact with the wall of one platelet will form the surface of the film on the following platelet. A schematic side view (as opposed to the front views shown previously) of a possible design is displayed in Fig. 5, where in a series of snapshots simulation results for the formation of a liquid film between the alternating platelets of 3.2 mm length are shown. The reactor housing is shown in gray, the reactor volume being filled with air (black) and ethanol (white). In such a design the liquid film is not guided inside grooves, but moves along the surface of the platelets. As an example, such a surface directed flow can be established by modifying the surface of the platelets and creating regions of different wettability, as reported in [5].

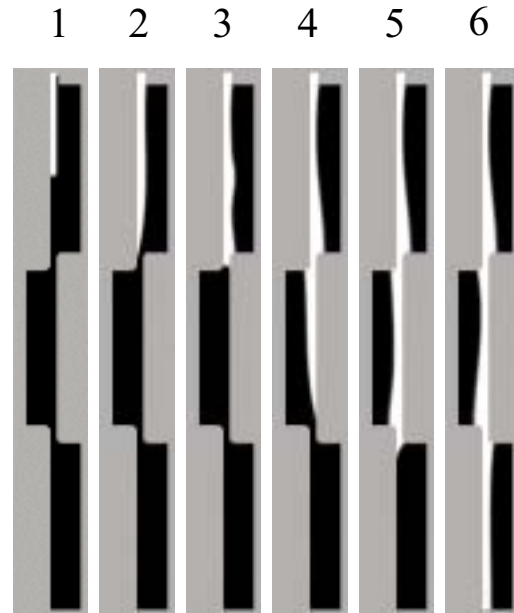


Figure 5: Formation of an ethanol film (in white) in a falling film reactor with alternating plates.

For the simulation of liquid film formation in the reactor, a 2D model based on the volume-of-fluid (VOF) method [6] was set up. Standard UPWIND and SIMPLEC schemes were used for the momentum and mass conservation equations, respectively. For surface reconstruction, the PLIC scheme was used [7]. The simulations were performed with the commercial flow solver CFD-ACE+ by CFDRC. A contact angle of ethanol with the solid material of  $10^\circ$  was assumed at the vertical faces limiting the reactor volume. In order to ensure that only the vertical faces are wetted by the liquid, a  $90^\circ$  contact angle was assigned to the horizontal faces. At the inlet, appearing as the small pipe on top of the geometry, a flow velocity of 2 cm/s and an ethanol volume fraction of 1 were prescribed. A body force equivalent to a gravitational acceleration of  $9.81 \text{ m/s}^2$  was set.

From Fig. 5 it can be seen that the reactor is filled with liquid and a film of 100-200  $\mu\text{m}$  thickness is formed. The film alternately contacts the left and the right row of

platelets. The varying thickness is mainly due to the  $90^\circ$  contact angle assigned to the horizontal faces. By choosing a higher contact angle the liquid is repelled more strongly, thus resulting in a more uniform film thickness. However, large contact angles tend to introduce numerical fluctuations, manifesting themselves in capillary waves travelling along the gas/liquid interface.

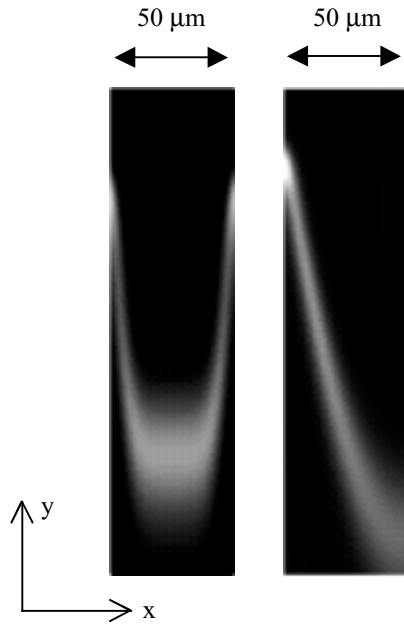


Figure 6: Dispersion of a concentration signal inside a liquid film in a reactor with alternating platelets (left) and with a single reaction plate (right).

The VOF simulations suggest that a suitable liquid film is formed in a reactor geometry with alternating platelets. In order to study hydrodynamic dispersion inside such a reactor, a simplified one-phase model was set up. When the length of a single platelet is very small (in the  $\mu\text{m}$  range) and wetting properties of the faces are appropriately chosen, the interfacial regions between gas and liquid will be planar. In such an arrangement the liquid can be driven by a pressure difference as well as by gravitation. Pressure as a driving force will result in a pressure difference between gas and liquid, which, however, is balanced by the Laplace pressure of the slightly curved interfacial regions each of which has an extension in flow direction of only a few  $\mu\text{m}$ . Hence, a 2D model was set up with a rectangular flow domain embracing the liquid phase only. For the regions where the liquid is in contact with a wall, no-slip boundary conditions were chosen, the gas/liquid interfaces were modeled by symmetry boundary conditions. A reactor geometry with non-overlapping platelets of only  $1\ \mu\text{m}$  extension and a film thickness of  $50\ \mu\text{m}$  was assumed. The solution algorithms were the same as discussed in the previous section. At the inlet, a flow velocity of  $2\ \text{cm/s}$  was prescribed.

In Fig. 6 it can be seen that in a reactor with  $1\ \mu\text{m}$  platelets arranged on the right and on the left side of the flow domain (not shown in the figure), the tracer signal, initialized at constant  $y$ , assumes the shape of a plug travelling in negative  $y$  direction. For comparison, the signal obtained in a reactor with a single plate on the left side of the flow domain is much more spread out. The signal shape obtained in the reactor with alternating platelets can be traced back to the corresponding velocity profile, which has an approximate plug-flow character.

## 4 DISCUSSION AND OUTLOOK

After significant spreading of concentration signals was proven for the state-of-the-art falling film reactor, it was shown that hydrodynamic dispersion can be reduced with an alternative design comprising alternating platelets being wetted by the liquid film. When the ratio of film distance and length of the platelets is varied, a number of different velocity profiles are found, as an example of which the plug-flow scenario was discussed in the previous section. An advantage of a design with platelets in the  $\mu\text{m}$  range is the fact that the liquid can be driven with pressure in addition to gravity, thus allowing even thin films to flow comparatively fast. Such a decoupling of residence time from film thickness gives much more flexibility in reactor operation as with purely gravity-driven films. Reducing the film thickness has yet another advantage: According to the theory of Taylor and Aris [8], dispersion in thin films is dominated by diffusion. Bearing in mind that diffusion in liquids is slow, thin films will allow an excellent control of residence time. In addition to that, it suggests itself that the alternating platelets induce a permanent entrance flow effect when their extension is small compared to a typical hydrodynamic or thermal entrance length. Thus, heat and mass transfer rates into the liquid film should be increased compared to the conventional design. This aspect will be investigated in future studies.

## REFERENCES

- [1] V. Hessel, W. Ehrfeld, K. Golbig et al., Proc. of IMRET3, Springer-Verlag, 526-540, 2000.
- [2] V. Haverkamp, V. Hessel, H. Löwe et al., Proc. of IMRET5, Springer-Verlag, to be published, 2002.
- [3] B.P. Leonard in: C. Taylor, W.G. Habashi, M.M. Hafez (Eds.), "Numerical Methods in Laminar and Turbulent Flow", Vol. 5, Part 1, 35-47, 1987
- [4] B. Noll, "Numerische Strömungsmechanik", Springer-Verlag, 1993
- [5] B. Zhao, J.S. Moore and D.J. Beebe, Science 291, 1023-1026, 2001
- [6] C.W. Hirt and B.D. Nichols, Journal of Computational Physics 39, 201-225, 1981
- [7] D.B. Kothe, W.J. Rider, S.J. Mosso et al., AIAA Paper, 96-08059
- [8] R. Aris, Proc. Roy. Soc. A235, 67-77, 1956

